PHYSICAL REVIEW B VOLUME 40, NUMBER 8 15 SEPTEMBER 1989-I

Fluorescence spectra of the layered semiconductor compound $MnPS_3$

V. Grasso, F. Neri, and L. Silipigni
Istituto di Struttura della Materia, Università degli Studi di Messina, Salita Sperone 31, Casella Postale 57, I-98166 Sant' Agata (Messina), Italy

M. Piacentini
Dipartimento di Energetica, Prima Università degli Studi di Roma, La Sapienza, I-00161 Roma, Italy
(Received 3 May 1989)

Fluorescence measurements on $MnPS_3$ layered semiconductor crystals, in the visible region, below their fundamental absorption thresholds, were carried out at room temperature. The resulting emission spectra show four overlapping structures, which fall in the region of intraion transitions for the Mn^{2+} $3d^5$ configuration. The results, deduced from deconvolution of the bands, agree well with those obtained from optical-absorption measurements and furthermore confirm the Mn^{2+} $3d$ energy-level distribution derived from the transition-metal weakly interacting model. From the analysis of the excitation spectrum for the $MnPS_3$ fluorescence band centered at 2.23 eV, additional information about the Mn^{2+} $3d$ excited-energy-state distribution and a verification of the validity of the above model are obtained.

INTRODUCTION

The two-dimensional compounds have always been a subject of widespread interest because of their original physical and chemical properties, and a great number of materials have been studied by many researchers. Among them, the large family of layered semiconducting MPS_3 compounds (where M is a first-row transition metal with an incomplete "d" shell) appears very intersting because of their possible, topotactic and reversible intercalation reactions, involving host-guest redox processes.[1–4] These intercalation compounds may be used, for example, with strongly electropositive alkali metals, (e.g., lithium), as electrode materials for high-energy secondary batteries.[5] In particular, $MnPS_3$ shows a rather uncommon behavior towards the intercalation process, whose origin has not yet been entirely understood. In fact, this compound seems to be easily intercalated by the pyridine molecules,[6] while it appears almost inert when the chemical Li intercalation is attempted.[3] Besides, the electrochemical Li intercalation does not lead to satisfactory results, showing an irreversible functioning for the Li_xMnPS_3 compounds which, therefore, do not seem to be good candidates as cathode materials in Li^+ transport secondary batteries.[7,8]

While the crystal structure,[9] and the optical and magnetic properties[6,10–12] of $MnPS_3$ are known, a detailed study of the $MnPS_3$ electronic band structure is missing, as for all MPS_3 compounds. Such an investigation is necessary to understand the origin of the different behavior upon intercalation. Besides that, a systematic analysis of pure $MnPS_3$ fluorescence spectra, at least to our knowledge, has not been reported in the literature, even if manganese is known to be an efficient luminescence activator in a number of host lattices, for example in ZnS.[3] In the room-temperature emission spectra of such a compound an orange emission band peaking at about 2.12 eV has been observed, and it is usually attributed to the ${}^4T_1({}^4G)\rightarrow{}^6A_1({}^6S)$ transition of the divalent manganese ion in the zinc sulfide crystal field.[13] Moreover, in the excitation spectrum of the orange emission band, five direct excitation subbands (at 3.19, 2.9, 2.65, 2.51, and 2.34 eV) have been noticed and it was supposed[14] that these bands are due to the transitions from the ${}^6A_1(S)$ ground state to the excited state of the divalent manganese ion in the zinc sulfide crystals, i.e., to the ${}^4E({}^4D)$ or ${}^4T_2({}^4D)$, ${}^4T_1({}^4P)$, ${}^4E({}^4G)$ and ${}^4A_1({}^4G)$, ${}^4T_2({}^4G)$ and ${}^4T_1({}^4G)$ states.

In this paper, we examine the fluorescence spectra of the $MnPS_3$ crystalline compound in the visible region, below its fundamental absorption thresholds. The interpretation of the resulting emission spectra confirms the Mn $3d$ energy-level distribution, derived from the transition-metal weakly interacting model,[15] and agrees well with the one given for the optical-absorption spectra.[10] We also analyze the room-temperature $MnPS_3$ excitation spectrum for the 2.23-eV Mn^{2+} fluorescence band. The peak positions of both the emission and excitation spectra, derived by the spectral deconvolution, allow us to calculate the so-called B and C Racah parameters.[16] Their values, related to the Coulomb repulsion between $3d$ electrons, provide another support to the above energy-level distribution model.

EXPERIMENTAL

The single crystals of $MnPS_3$, used in this work, were grown and supplied by R. Brec of the Laboratoire de Chimie des Solides, Université de Nantes. These samples are transparent, green, hexagonal plates. They are 3.5 mm long and 3 mm wide, while their thickness changes from 0.014 to 0.05 mm. The emission and excitation spectra have been measured in the visible region, using a

Perkin-Elmer fluorescence spectrophotometer (model 650-40). Fluorescence has been excited by a 150-W Xe lamp, and it has been measured at an angle less than 45° to the exciting light in a transmission geometry. In order to eliminate higher-order components of the excitation wavelength, which could occur in the spectra, different filters have been interposed between the excitation monochromator slit and the samples. The wavelength accuracy was ±2 nm. All measurements have been carried out at room temperature and have been repeated several times in order to check their reproducibility.

To maximize the accuracy of the measurements, a portion of the excitation light, diverted by a beam splitter to a reference detector, has been employed as a feedback signal to correct any fluctuation in source lamp intensity. To prevent any errors due to zero shifting, we have automatically zeroed the spectrofluorometer immediately after initialization and periodically checked its automatic zero setting from then on.

RESULTS

Figures 1–3 show the room-temperature emission spectra of $MnPS_3$, measured between 2.1 and 2.8 eV, for three different excitation energies. They are represented by the solid line. Four reproducible emission structures are present in them. In fact, these spectra are dominated by a strong emission band peaking at about 2.54 eV, followed by a weak shoulder of lower intensity at about 2.64 eV. On the low-energy side, a broad asymmetric peak is visible at about 2.23 eV, followed by a wide shoulder at about 2.45 eV. Such a spectrum can be fairly well reproduced with four overlapping Gaussian bands. The least-squares-fitting procedure results, i.e., the parameters of the four overlapping Gaussian curves, are reported in Table I. In Figs. 1–3, the deconvoluted Gaussian curves are shown with the dotted lines, and the best fit calculated emission spectrum is represented by the dashed line. The emission band at about 2.23 eV is fairly characteristic of the Mn^{2+} ion when it is either octahedrally or tetrahedrally coordinated in a large variety of compounds.[17]

Furthermore, in order to get a comparison with the structures present in the absorption spectrum of $MnPS_3$ we measured the room-temperature excitation spectrum, monitoring the entire fluorescence band centered at about 2.23 eV. The results are reported in Fig. 4. Two features are observed at about 2.9 and 3.13 eV, besides those at 2.54 and 2.64 eV already noticed in the emission spectra.

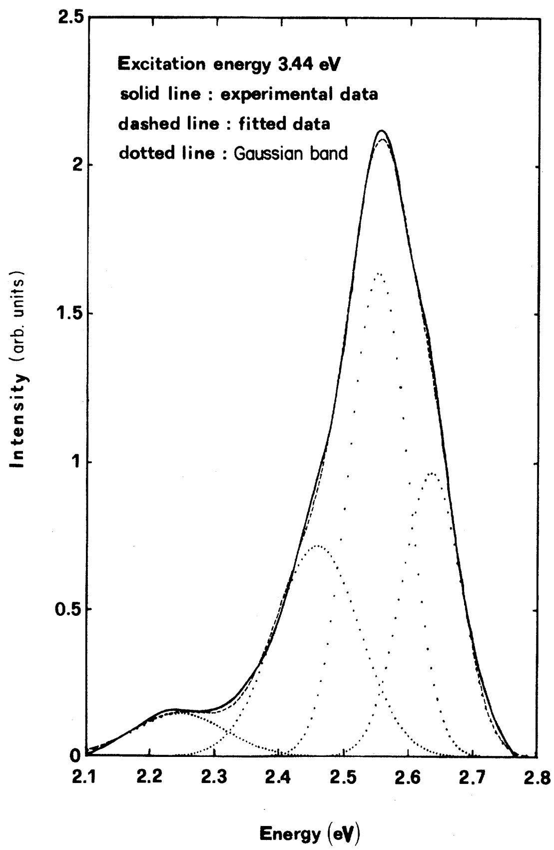

FIG. 1. Room-temperature emission spectra of $MnPS_3$, in the region of the Mn $3d$-$3d$ transitions (solid line) obtained by exciting at 3.44 eV. The dashed line is the best-fit calculated emission spectrum, while the dotted lines represent the deconvoluted Gaussian curves.

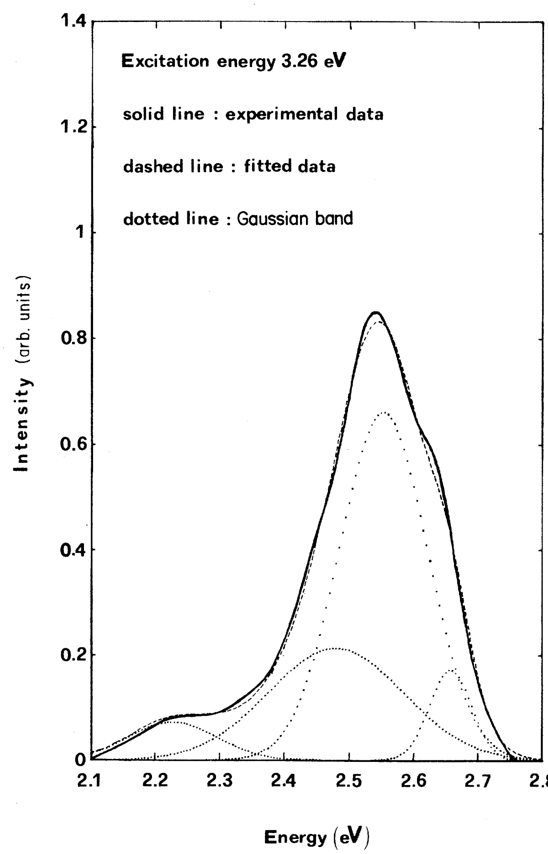

FIG. 2. Room-temperature emission spectra of $MnPS_3$, in the region of the Mn $3d$-$3d$ transitions (solid line), obtained by exciting at 3.26 eV. The dashed line is the best-fit calculated emission spectrum, while the dotted lines represent the deconvoluted Gaussian curves.

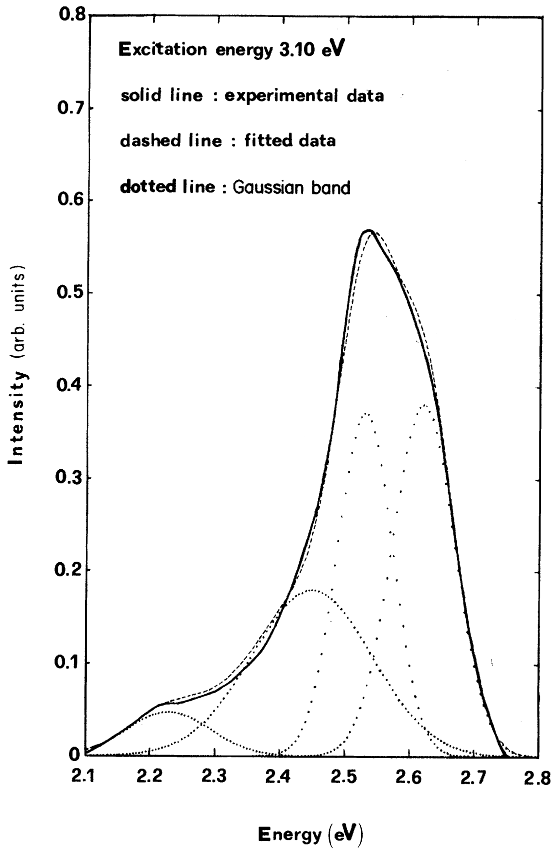

FIG. 3. Room-temperature emission spectra of $MnPS_3$, in the region of the Mn $3d$-$3d$ transitions (solid line), obtained by exciting at 3.10 eV. The dashed line is the best-fit calculated emission spectrum, while the dotted lines represent the deconvoluted Gaussian curves.

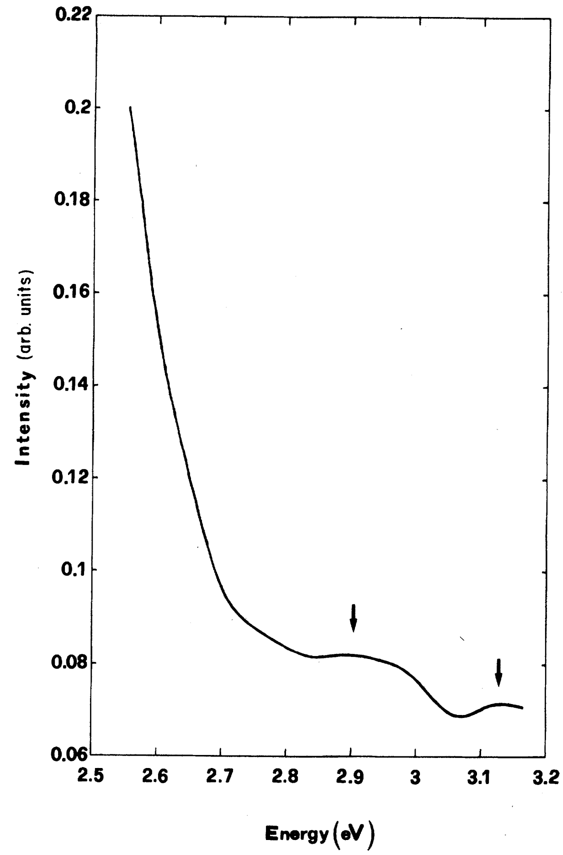

FIG. 4. Room-temperature excitation spectrum of the $MnPS_3$ fluorescence band centered at 2.23 eV. The two observed structures at 2.9 and 3.13 are marked by arrows.

The two structures at about 2.9 and 3.13 eV are marked by arrows in Fig. 4. As will be seen in the following discussion, such features can be attributed to the Mn^{2+} ion.

DISCUSSION

Model

Experiments on x-ray photoemission,[18] absorption,[10,11] optical,[12,15,19,20] and electrical transport[21,22] properties were accomplished, leading to formulation of band models for some MPS_3 compounds. In particular, with the so-called M weakly interacting model,[15] where M is the transition metal, we have successfully interpreted, in previous papers, the electrical transport properties of $NiPS_3$ and $MnPS_3$ compounds.[21,22] Besides, such a model seems to explain very well the features of soft-x-ray valence-band spectra and of below-band-gap optical-absorption spectra of these compounds. Figure 5 shows the proposed simplified version of an energy-level scheme for $MnPS_3$ derived from the above model, which we will adopt to interpret the structures observed in the $MnPS_3$ fluorescence spectra.

TABLE I. Energies of the emission maxima E_0, heights of the maxima A (in arbitrary units), and half-widths at half maxima σ of the Gaussians $A\exp[-(\ln 2)(\hbar\omega-E_0)^2/\sigma^2]$, used to fit the emission bands observed in the fluorescence spectra of $MnPS_3$.

E_0 (eV)	A	σ (eV)
2.23	0.07	0.09
2.45	0.26	0.11
2.54	0.73	0.08
2.64	0.38	0.06

For the Mn^{2+} ion, the electron configuration is $(3d)^5$. When the ligands (chalcogens in $MnPS_3$) are placed in octahedral positions about such an ion, like in $MnPS_3$ compound, the degenerate $3d$ orbitals, in which the single d electron is accommodated, split to give rise to a set of lower-energy t_{2g} orbitals and a set of higher-energy e_g orbitals.[23] Furthermore, in a high-spin octahedrally coordinated Mn^{2+} complex, the lowest configuration $(t_{2g}^3e_g^2)$ gives rise to the ground state ${}^6A_{1g}({}^6S)$, possessing five unpaired spins. The first four excited states will come from the free-ion ${}^4G$ state, while the immediately successive ones will come from the free-ion ${}^4D$ state. Transitions from the ground state to those excited states, which are formed by spin reversal, would be normally forbidden. However, since the crystalline field perturbs the pure states, a loosening of the selection rules occurs. In fact, in an octahedral field, the ^4D state of the free ion splits into a twofold-degenerate state $^4E_g(t_{2g}^3e_g^2)$ and a threefold-degenerate state $^4T_{2g}(t_{2g}^3e_g^2)$, while the ^4G state of the free ion splits into a nondegenerate state $^4A_{1g}(t_{2g}^3e_g^2)$, a doubly degenerate state $^4E_g(t_{2g}^3e_g^2)$, and two triply degenerate states $^4T_{1g}(t_{2g}^4e_g^1)$ and $^4T_{2g}(t_{2g}^4e_g^1)$.[24] In the absence of any distortion of an octahedral field, the levels $^4A_{1g}$ and ^4E_g would be degenerate. Nevertheless, in Fig. 5, we have represented such degenerate levels by two different states because we have allowed for their already observed splitting.[10,25,26] In fact, the degeneracy predicted in the cubic approximation is removed by the trigonal field.[27] In Fig. 5 A and B denote the valence bands arising from the $3p_xp_y$ hybridization of P and S atomic orbitals and from the $3p_z$ bonding orbitals of the P-P pair, respectively; while E and F represent the lowest conduction states consisting of $3p_z^*$ antibonding orbitals of S and P.

If the octahedron of the chalcogens is distorted along the trigonal axis, then a further splitting of the octahedral levels takes place and the symmetry of the compound is lowered from O_h to D_{3d}. In such a case, the trigonal field does not remove the twofold degeneracy of the level E_g, while it splits each triply degenerate level (T_{1g} or T_{2g}) into a doubly degenerate (E_g) and a nondegenerate (A_{2g} or A_{1g}) level.[24]

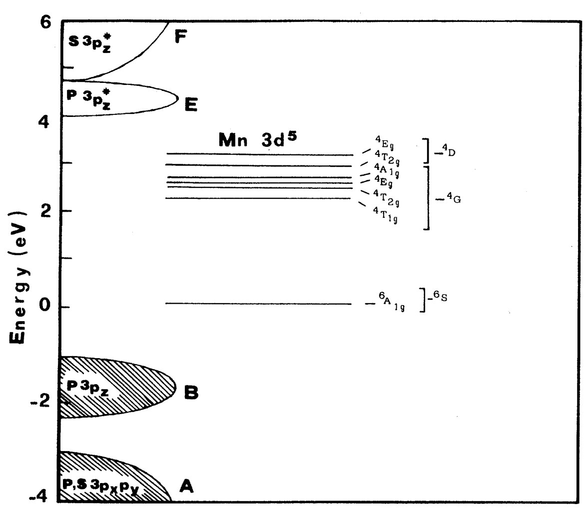

FIG. 5. Simplified version of the energy-level scheme adopted to describe the electronic structure of $MnPS_3$. A and B denote the valence bands arising from the $3p_xp_y$ hybridization of P and S, and from the $3p_z$ bonding orbitals of P-P, respectively. E and F represent the lowest conduction states consisting of $3p_z^*$ antibonding orbitals of S and P. $^6A_{1g}$ denotes the ground state of the Mn^{2+} d^5 electronic configuration in the crystal, while $^4T_{1g}(^4G)$, $^4T_{2g}(^4G)$, $^4E_g(^4G)$, $^4A_{1g}(^4G)$, $^4T_{2g}(^4D)$, and $^4E_g(D)$ represent the excited states. The energy values are referred to the Fermi energy level, which is assumed to coincide with $^6A_{1g}$ level (Ref. 19).

Mn^{2+} emission in $MnPS_3$

The observed structures in the emission spectra of several $MnPS_3$ layered semiconductor crystals can be qualitatively interpreted, in the framework of the ligand-field theory, as transitions between the $3d$ levels of the Mn^{2+} ion, which are split by the crystal field of the surrounding chalcogens. In fact, at photon energies close to or less than the band gap of this compound (typically from 1.5 to 3.5 eV), very weak $3d$-$3d$ transitions on the transition-metal ion occur.[10] Moreover, these transitions, because of their weak oscillator strength, cannot give significant structures above the absorption threshold.

For the assignment of the emission bands, we refer to a previous paper,[10] in which the optical-absorption spectra of $MnPs_3$ are reported, following the calculations given by Orgel[28] in the weak-crystal-field approximation. In fact, by comparison with these optical spectra, we ascribe the four peaks at 2.23, 2.45, 2.54, and 2.64 eV to the transitions from the quartet $^4T_{1g}$, $^4T_{2g}$, ^4E_g, and $^4A_{1g}$ excited states to the $^6A_{1g}$ ground state, having allowed for the observed splitting of the originally degenerate $^4A_{1g}$ and ^4E_g levels. The former two transitions have an interconfigurational character:

$$t_2^ne^m \rightarrow t_2^{n-k}e^{m+k} \text{ with } k=-1 ,$$

while the latter two transitions have an intraconfigurational character. These bands occur in the emission spectra at greater energy values than those reported in the optical-absorption spectra. However, such an apparent disagreement can be explained by considering the half-width values of the Gaussian curves obtained from fitting of the absorption peaks of the Mn $3d$-$3d$ transitions in $MnPS_3$.[10] In fact if we consider, for example, the half-width value of the absorption peak centered at about 1.93 eV, it is about double that obtained by us for the corresponding emission peak. Therefore, the emission-peak energy position falls well within the half-width values of the corresponding absorption peaks, allowing us to attribute the observed emission peaks to the above transitions.

In the bidimensional approximation, the crystal symmetry of $MnPS_3$ is represented by the D_{3d} space group. When such a symmetry is present, on the basis of the selection rules for both the electric and magnetic dipole induced transitions, these transitions, with either xy or z polarization, are allowed.[24,29,30] However, in general, the probability of a magnetic dipole transition is approximately $(137)^2$ weaker than the electric dipole transition.[31] For this reason, even a small breakdown in the parity selection rule allows the electric dipole transitions to dominate[24]. This accounts for why the $^4E_g \rightarrow {}^6A_{1g}$, $^4A_{1g} \rightarrow {}^6A_{1g}$ and $^4T_{2g} \rightarrow {}^6A_{1g}$ transitions are more intense than the $^4T_{1g} \rightarrow {}^6A_{1g}$ transition.

Furthermore, we have observed the splitting of the originally degenerate $^4A_{1g}$ and ^4E_g levels. Such a splitting has already been deduced from the analysis of the optical-absorption spectrum of $MnPS_3$,[10] with the aid of the Koide and Pryce curves, showing the variation of the $^4A_{1g}$ and ^4E_g energy levels as a function of the covalency parameter: the $^4A_{1g}$ level was higher than the doubly degenerate ^4E_g level by about 60 meV.[25] From our measurements we obtain a splitting of about 100 meV. According to the calculations of Koide and Pryce,[25] the observed splitting of the originally degenerate $^4A_{1g}$ and ^4E_g levels could be due to an increase in the covalency existing in the Mn compounds. Besides that, also a distortion of octahedral field around Mn^{2+} ions could cause a significant splitting between the $^4A_{1g}$ and ^4E_g levels. As will be seen in the following section, the $MnPS_3$ excitation spectrum analysis shows that in this compound the Mn—S bonding has a high degree of ionicity. Therefore, the presence of such a fine substructure in the Mn $3d$ states is more likely to be attributed to the trigonal distortion of the octahedral field around the Mn^{2+} ions, caused by a not well-matching value of the monoclinic unit cell angle β,[32] rather than to an increase in covalency of bonding.

Mn^{2+} excitation in $MnPS_3$

On the basis of the ligand-field theory the structure at about 3.19 eV, observed in the excitation spectrum of the orange emission band of ZnS:Mn, was attributed to the transitions from the $^6A_{1g}(^6S)$ ground state to the $^4E_g(^4D)$ or $^4T_{2g}(^4D)$ states.[13] Following this interpretation and referring to the energy-level diagram for the Mn^{2+} ion in octahedral coordination, given by Orgel,[28] the 2.9 and 3.13 eV structures in the excitation spectrum for the 2.23 eV $MnPS_3$ fluorescence band can be attributed to transitions between the quartet $^4T_{2g}(^4D)$ and $^4E_g(^4D)$ excited states and the $^6A_{1g}(^6S)$ ground state, respectively (see Fig. 5). The energy-level diagram[28] shows only the positions of the lowest quartet levels as a function of the crystal field strength, Dq, in the octahedral symmetry. Such a diagram is, as usual, a function of three parameters: Dq and the so-called Racah coefficients B and C.[33] All the free-ion energy levels, which arise from a fixed number of d electrons, can be described by just two constants B and C, known as the Racah parameters.[16] These Racah coefficients are linear combinations of the Slater-Condon integrals F_2 and F_4 for atomic spectra. In particular, for d electrons, the interelectronic repulsion parameters B and C are related to the integrals F_2 and F_4 by the following expressions:[34]

$$B = F_2 - 5F_4 \quad \text{and} \quad C = 35F_4 \ ,$$

Although none of the two electrostatic interaction parameters B and C have a directly interpretable physical significance, it has been observed that the B values reduces in covalent compounds.[35] A change of the B value from that of the free ion will, therefore, supply information on the degree of ionicity of bonding between manganese and the six sulfur ligands in $MnPS_3$. Since the energy differences

$$[E(^4E_g(^4D)) - E(^6A_{1g}(^6S))]$$

and

$$[E(^4A_{1g}(^4G)) - E(^6A_{1g}(^6S))]$$

are independent of the Dq value, the corresponding excitation and emission bands are particularly suited for the calculation of the B and C values. For the electronic configuration d^5 they obey the following equations:[16,25,34]

$$10B + 5C = E(^4A_{1g}(^4G)) \ ,$$

$$17B + 5C = E(^4E_g(^4D)) \ ,$$

where $E(^4A_{1g}(^4G))$ and $E(^4E_g(^4D))$ are the energies of the $^4A_{1g}(^4G)$ and $^4E_g(^4D)$ states measured from the gorund state $^6A_{1g}(^6S)$, i.e., equal to 2.64 and 3.13 eV, respectively, as deduced from the $MnPS_3$ emission and excitation spectra. In the above equations the free-ion ground term ^6S has been subtracted.[34] Thus, we obtain $B = 600\ \text{cm}^{-1}$ and $C = 3150\ \text{cm}^{-1}$.

In Table II the values of the Racah B and C parameters, for an octahedrally coordinated Mn^{2+} ion in various manganese compounds, are listed. The B and C value, derived for $MnPS_3$ in this work, agree well with those obtained for the Mn^{2+} free ion and other Mn ionic compounds. In particular the resulting B value, being only slightly lower than that of the free ion, bears out the validity of the transition-metal weakly interacting model for the interpretation of the electronic properties of this layered semiconductor compound.

CONCLUSION

From the analysis of the room-temperature fluorescence spectra of the $MnPS_3$ compound in the visible region, below the fundamental absorption threshold, the followings information can be drawn.

Some structures have been observed and attributed to the Mn $3d$-$3d$ transitions on the basis of the ligand-field theory.

The position of the Mn^{2+} $3d$ excited energy levels with respect to the ground state, derived from the optical-absorption spectra, has been confirmed.

The existence of a fine splitting of about 100 meV has been revealed in the originally degenerate $^4A_{1g}$ and ^4E_g levels. The presence of such a splitting has already been shown from optical-absorption measurements.[10]

TABLE II. The Racah B and C parameters for the octahedrally coordinated Mn^{2+} ion in different compounds.

Mn^{2+} in	B (cm^{-1})	C (cm^{-1})	Ref.
Free ion	786	3790	a
MnO	786	3210	a
MnS	583	3125	b
$MnCl_2 \cdot 2H_2O$	630	3600	c
$MnPS_3$	600	3150	present work

[a] G. W. Pratt and R. Coelho, Phys. Rev. **116**, 281 (1959).
[b] F. A. Kroger, Physica **7**, 92 (1940).
[c] K. E. Lawson, J. Chem. Phys. **44**, 4159 (1966).

Analyzing the excitation spectrum for the emission band at 2.23 eV, additional information about the distribution of the Mn^{2+} $3d$ excited energy levels with respect to the ground state have been obtained.

The resulting $MnPS_3$ Racah parameter B value agrees well with those obtained for the Mn^{2+} free ion and other Mn ionic compounds.

All the above considerations strongly support the hypothesis that the transition-metal weakly interacting model[15] is adequate for interpreting most of the electronic properties of this material.

[1]M. Barj and G. Lucazeau, Solid State Ionics **9/10**, 475 (1983).

[2]J. P. Audier, R. Clement, Y. Mathey, and C. Mazieres, Physica B+C **99B**, 133 (1980).

[3]R. Brec, D. M. Schleich, G. Ouvrard, A. Louisy, and J. Rouxel, Inorg. Chem. **18**, 1814 (1979).

[4]A. Le Mehaute, G. Ouvrard, R. Brec, and J. Rouxel, Mater. Res. Bull. **12**, 1191 (1977).

[5]M. S. Whittingham, Prog. Solid State Chem. **12**, 41 (1978).

[6]K. Okuda, K. Kurosawa, S. Saito, M. Honda, Z. Yu, and M. Date, J. Phys. Soc. Jpn. **55**, 4456 (1986).

[7]R. Brec, G. Ouvrard, A. Louisy, J. Rouxel, and A. Le Mehaute, Solid State Ionics **6**, 185 (1982).

[8]A. Le Mehaute, G. Ouvrard, R. Brec, and J. Rouxel, Mater. Res. Bull. **12**, 1191 (1977).

[9]W. Klingen, G. Eulenberger, and H. Hahn, Z. Anorg Allog. Chem. **401**, 97 (1973).

[10]V. Grasso, S. Santangelo, and M. Piacentini, Solid State Ionics **20**, 9 (1986).

[11]V. Grasso, S. Santangelo, and M. Piacentini, Solid State Commun. **60**, 381 (1986).

[12]F. S. Khumalo and H. P. Hughes, Phys. Rev. B **23**, 5375 (1981).

[13]L. Ozawa, R. Husimura, and Y. Ato, in *Proceedings of the International Conference on Luminescence, Budapest, 1966,* edited by G. Szipeti (Akadémiai Kiadó, Budapest, 1968), Vol. 1, p. 1177.

[14]A. I. Ryskin, G. I. Khilko, B. I. Maksakov, and K. K. Dubenskii, Opt. Spektrosk. **16**, 274 (1964) [Opt. Spectrosc. (USSR) **16**, 149 (1964)].

[15]M. Piacentini, F. S. Khumalo, C. G. Olson, J. W. Anderegg, and D. W. Lynch, Chem. Phys. **65**, 289 (1982).

[16]G. Racah, Phys. Rev. **62**, 438 (1942).

[17]L. E. Orgel, J. Chem. Phys. **23**, 1958 (1955).

[18]M. Piacentini, F. S. Khumalo, G. Levêque, C. G. Olson, and D. W. Lynch, Chem. Phys. **72**, 61 (1982).

[19]M. Piacentini, V. Grasso, S. Santangelo, M. Fanfoni, M. Modesti, and A. Savoia, Solid State Commun. **51**, 467 (1984).

[20]M. Piacentini, V. Grasso, S. Santangelo, M. Fanfoni, S. Modesti, and A. Savoia, Nuovo Cimento **D4**, 444 (1984).

[21]V. Grasso, F. Neri, S. Santangelo, L. Silipigni, and M. Piacentini, Phys. Rev. B **37**, 4419 (1988).

[22]V. Grasso, F. Neri, S. Santangelo, L. Silipigni, and M. Piacentini, J. Phys. Condensed Matter **1**, 3337 (1989).

[23]Gordon M. Barrow, *Introduction to Molecular Spectroscopy* (McGraw-Hill, New York, 1962), p. 293.

[24]M. Tinkham, *Group Theory and Quantum Mechanics* (McGraw-Hill, New York, 1964), Chap. 4.

[25]S. Koide and M. H. L. Pryce, Philos. Mag. **3**, 607 (1958).

[26]R. Pappalardo, Philos. Mag. **2**, 1397 (1957).

[27]J. Pollini, G. Spinolo, and G. Benedek, Phys. Rev. B **22**, 6369 (1980).

[28]L. E. Orgel, J. Chem. Phys. **23**, 1004 (1955).

[29]R. Englman, *The Jahn-Teller Effect in Molecules and Crystals* (Wiley-Interscience, London, 1972), p. 302.

[30]L. D. Landau and E. M. Lifshitz, Vol. 3 of *Course of Theoretical Physics: Quantum Mechanics* (Pergamon, London, 1958), Chap. 12.

[31]C. J. Ballhausen, *Introduction to Ligand Field Theory, McGraw-Hill Series in Advanced Chemistry* (McGraw-Hill, New York, 1962), p. 33.

[32]R. Brec, G. Ouvrard, A. Louisy, and J. Rouxel, Ann. Chim (Paris) **6**, 499 (1980).

[33]Y. Tanabe and S. Sugano, J. Phys. Soc. Jpn. **9**, 753 (1954).

[34]N. Bruce Hannay, *Treatise on Solid Chemistry,* edited by N. Bruce Hannay (Plenum, New York, 1975), Vol. 2.

[35]D. L. Wood, in *Optical Properties of Solids,* edited by S. Nudelman and S. S. Mitra (Plenum, New York, 1969), Chap. 19, p. 576.